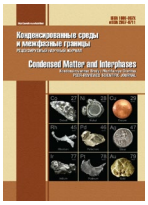

ISSN 1606-867X (Print)
ISSN 2687-0711 (Online)
Condensed Matter and Interphases
Kondensirovannye Sredy i Mezhfaznye Granitsy
https://journals.vsu.ru/kcmf/

Original articles

Research article
https://doi.org/10.17308/kcmf.2022.24/9057

Effect of the morphology and composition of trimetallic PtCuAu/C catalysts on the activity and stability of the methanol oxidation reaction

V. S. Menshchikov✉, S. V. Belenov, A. Yu. Nikulin

Southern Federal University,
105/42 Bolshaya Sadovaya str., Rostov-on-Don 344006, Russian Federation

Abstract

A study on the influence of the method for obtaining trimetallic PtCuAu/C catalysts on their activity in the oxidation of methanol has been carried out.

The structural characteristics of the obtained trimetallic catalysts have been studied by X-ray diffraction and transmission electron microscopy. The nanoparticles of the material obtained by the galvanic synthesis method had a size twice as large (~ 6 nm) than the nanoparticles of the material obtained by the co-deposition of metal precursors. According to the results from the accelerated stress testing of catalysts, it was found that the material obtained by the galvanic method of substitution of copper atoms with gold had a higher residual activity in the oxidation of methanol than the commercial Pt/C analogue.

This study shows the potential of obtaining and using multicomponent platinum-containing nanoparticles deposited on a carbon carrier as effective catalysts for use in methanol fuel cells.

Keywords: methanol fuel cells, catalysis, trimetallic catalysts, galvanic replacement

Funding: The reported study was supported by the Russian Foundation for Basic Research, project no. 19-33-90140.

Acknowledgements: The authors are grateful to LLC “Systems for Microscopy and Analysis” (Skolkovo, Moscow) for conducting TEM and EDX studies.

For citation: Menshchikov V. S., Belenov S. V., Nikulin A. Yu. Effect of the morphology and composition of trimetallic PtCuAu/C catalysts on the activity and stability of the methanol oxidation reaction. *Kondensirovannye sredy i mezhfaznye granitsy = Condensed Matter and Interphases*. 2022;24(1): 76–87. https://doi.org/10.17308/kcmf.2022.24/9057

Для цитирования: Меньщиков В. С., Беленов С. В., Никулин А. Ю. Влияние структуры триметаллических катализаторов на активность и стабильность в реакции окисления метанола. *Конденсированные среды и межфазные границы*. 2022;24(1): 76–87. https://doi.org/10.17308/kcmf.2022.24/9057

✉ Vladislav S. Menshikov, e-mail: men.vlad@mail.ru

1. Introduction

The study of the methanol oxidation reaction (MOR) is of great practical importance for the commercialization of direct methanol fuel cells (DMFC). Despite numerous studies in the field of DMFC, their widespread use is hindered by several factors: the slow methanol oxidation reaction, the poisoning of the catalytic layer by intermediate oxidation products, and the high cost of the catalysts themselves containing noble metals. These problems are relevant for both an anode catalyst of methanol oxidation [1] and a cathode oxygen reduction catalyst. At the same time, another important problem of cathode catalysts is the crossover of methanol into the cathode space [2]. Pt nanoparticles deposited on a finely dispersed carbon carrier are one of the most common catalysts; however, the rather high cost of this metal, combined with its low tolerance to intermediate oxidation products, remains the main problem preventing the widespread use of Pt as an anode and/or cathode in DMFC.

The mechanism of methanol oxidation in an acidic medium can be represented as a sequence of several stages [3].

1. Electro adsorption of methanol molecules on a Pt electrode followed by the formation of intermediate products such as -CHO, -COOH, -CO, etc.

2. The formation of Pt-OH on the catalyst surface because of water decomposition followed by the participation of hydroxyl groups in the oxidation of intermediate products.

3. Removal of formed CO_2.

Among the intermediate products of methanol oxidation, CO is the most harmful. CO molecules are chemisorbed on the surface of the Pt catalyst, which leads to blocking of active surface areas and reduces the activity of the catalyst. One of the possible ways to solve this problem is to change the electronic structure of the metal by doping the Pt catalyst with various noble (Pd, Ru, Au) and some transitional *d*-metals (Cu, Ni, Fe, Co, etc.), which contribute to the removal of CO from the surface, facilitating its oxidation to CO_2 [4–6]. PtRu alloys are well-known catalysts with a lower sensitivity to CO compared to pure Pt [7–8]. However, due to the relatively high cost of the Ru doping component, the most relevant are catalysts doped with transition *d*-metals, such as PtNi [9], PtCu [10], PtCo [10–11].

Thus, the authors of [10] showed that the obtained PtCo/C and PtCu/C catalysts demonstrated higher activity in the oxidation reaction, compared to PtRu/C. At the same time, the authors of the study noted that in the process of standardization (activation) of the surface, the doping component can be dissolved from the catalyst surface, and copper ions passing into the electrolyte can distort the results of experimental studies.

It was shown in [4] that the doping of platinum with copper atoms increased the catalytic activity in the reactions of methanol oxidation and oxygen reduction by 5 and 2 times, respectively, compared to Pt/C. The positive influence of the doping component on the activity of Pt catalysts can be explained by two effects. The first is a bifunctional mechanism of catalysis, in which the high rate of methanol oxidation is determined by the easier adsorption of OH groups on the surface of the doping component, which in turn led to the faster oxidation of chemisorbed CO molecules on neighbouring areas of the Pt surface [12]. The second is the electronic effect associated with the electronic interaction of the atoms of the doping component with Pt atoms. This effect leads to a decrease in the binding energy of adsorbed particles with the catalyst surface. As we mentioned earlier, the main disadvantage of bimetallic PtCu/C catalysts is the possible selective dissolution of the doping component during their functioning [10]. Over the past two years, the preparation and modification of bimetallic PtCu/C catalysts has been an urgent task for researchers around the world. In addition, more and more groups are focusing on the preparation and study of trimetallic nanoparticles (NP) containing Cu: PtCuNi [13], PtCuAu [14], PtPdCo [15], PtCuCo [16], etc. Earlier, it was shown [18–19] that the substitution of Cu atoms by Au atoms on the surface of a platinum-containing catalyst promotes not only an increase in the activity in MOR and the oxygen reduction reaction (ORR), but also a decrease in the selective dissolution of the doping component in the electrochemical cell. However, the question of the relationship between the structure, activity, and stability of trimetallic catalysts remains unclear.

The purpose of this study was the investigation of the relationship between the structure, activity in MOR and the stability of trimetallic PtCuAu/C catalysts obtained by various methods.

2. Experimental

Synthesis of trimetallic PtCuAu/C catalysts was carried out by two different methods. In the first case, the preparation of the catalyst was performed in two stages. At the first stage, a PtCu/C material with a solid solution structure and theoretical Pt:Cu ratio of 1:1 was obtained [18–19]. For this, the required amount of precursors of $H_2PtCl_6 \cdot 6H_2$ (Aurat, Russia, mass fraction of patina – 37.6%) and $CuSO_4 \cdot 5H_2O$ (analytical grade) were added to the water–ethylene glycol suspension of the Vulcan-XC72 carbon carrier in such a way that the mass fractions of metals will be 30 wt%. Pt and 10 wt%. Cu. Then, with constant stirring, an excess of 0.5 M $NaBH_4$ solution was added for joint reduction of Pt and Cu. This synthesis method is described in more detail in [20–21]. Further, after filtration and drying, a part of the PtCu/C catalyst obtained in the first stage was used in the second stage of synthesis. For this, a water–ethylene glycol solution was added to a weighed portion of the PtCu/C material, the resulting suspension was dispersed by ultrasound, and the calculated amount of the gold precursor $HAuCl_4 \cdot 4H_2O$ (Aurat, Russia, mass fraction of gold 49.04%) was added with constant stirring. The amount of gold precursor was calculated in such a way that at full reduction, the gold content in the resulting material was 5 at% of the metal phase. In this case, after the addition of the gold precursor, galvanic substitution of Cu atoms by Au atoms from the catalyst surface occurred. After keeping the suspension under constant stirring for 30 min the resulting suspension was filtered, washed several times with water and isopropyl alcohol, and then dried over P_2O_5. The resulting catalyst was labelled as PtCuAu/C_G.

Another method for the synthesis of the PtCuAu/C catalyst is based on the reduction of three metal with a $NaBH_4$ solution in water-ethylene glycol suspension [18–19]. In this case, the theoretical calculation of the mass fractions of metals corresponded to the PtCuAu/C_G material. This catalyst was labelled as PtCuAu/C_A.

The mass fraction of metals was determined by thermogravimetry based on the weight of the unburned residue. For this, the test sample was placed in a pre-calcined crucible with a constant weight and heat treated in a muffle furnace in an air atmosphere at 800 °C for 40 min. It should be considered that the unburned residue consists of Pt, Au, and CuO. The metal ratios of Pt:Cu and Pt:Cu:Au in the obtained catalysts was determined by X-ray fluorescence analysis (XRF) using a RFS-001 spectrometer (Research Institute of Physics, Southern Federal University, Russia). The conditions of the analysis were following X-ray tube voltage, 50 kV; current, 150 μA; anode material, molybdenum; spectrum acquisition time, 300 s. Registration and processing of X-ray fluorescence spectra was carried out using the UniveRS software (Southern Federal University, Russia) [22].

The phase composition of the materials and the average crystallite size were determined by powder X-ray diffraction at room temperature using ARL X'TRA diffractometer (CuK_α), within an angle range of 2θ from 15 to 55 degrees, with a step of 0.02 degrees and a registration rate of 2 degrees per minute. The average crystallite size was determined using the Scherrer formula [23]:

$$D = \frac{K\lambda}{\mathrm{FWHM} \cdot \cos\theta},$$

where $K = 0.98$ is the Scherrer constant, λ is the wavelength of monochromatic radiation in Å, FWHM is the full width of the peak at half maximum (in radians), D is the average crystallite size, nm; θ is the reflection angle in radians.

The study by transmission electron microscopy (TEM) was performed using a microscope JEM-2100 (JEOL). Samples of materials weighing 0.5 mg were placed in 1 ml of heptane, the resulting suspension was homogenized in ultrasound for 2–3 min and applied to a nickel mesh coated with a thin layer of amorphous carbon. The materials were studied by transmission electron microscopy (TEM), high-resolution transmission electron microscopy (HRTEM), and scanning transmission electron microscopy (STEM) using an energy dispersive X-ray (EDX) microanalysis of the elemental composition. The electrochemical behaviour of the catalysts was studied at room temperature on a rotating disk electrode in a three-electrode cell by cyclic voltammetry using

a VersaSTAT 3 potentiostat. A saturated silver chloride electrode with a potential of 0.208 V was used as a reference electrode. Later in the study, all potentials were recalculated relative to the potential of a reversible hydrogen electrode. For the application of the studied catalyst to the working electrode, catalytic ink was prepared according to the procedure described in [24]. For the preparation, a catalyst sample weighing 0.0060 g was placed in a mixture of 900 μL of isopropanol and 100 μL of 0.5% Nafion alcohol solution (DuPont). The resulting suspension was stirred on a magnetic stirrer for 10 min, and then dispersed by ultrasound for the same time, while monitoring the temperature of the catalytic ink, which did not rise above 25 °C [25–26]. The mixing procedure was repeated, and then a 6 μL aliquot of ink was applied to the end of the disk electrode, dried at 700 rpm at room temperature, while the surface of the disk electrode was preliminarily polished and degreased according to the manufacturer's recommendations.

The surface of the catalytic layer was standardized in 0.1 M $HClO_4$ saturated with Ar for 30 min in the potential range of 0.04–1.20 V with a potential sweep rate of 200 mV/s. After standardization, the electrolyte was replaced with freshly prepared 0.1 M $HClO_4$ (Sigma Aldrich) to exclude the influence of dissolved copper ions on the values of the measured characteristics. After that, the cell was again saturated with argon and the electrochemical surface area (ESA) was measured with a potential sweep rate of 20 mV/s. ESA values were calculated based on the electrochemical adsorption and desorption of hydrogen [27] using the formula:

$$\mathrm{ESA} = \frac{Q_\mathrm{H}}{R \cdot m},$$

where $Q_\mathrm{H} = \frac{(Q_\mathrm{ad} + Q_\mathrm{des})}{2}$ is the average amount of electricity used for the electrochemical adsorption and desorption of hydrogen; R is the amount of electricity used for the adsorption/desorption of a monolayer of atomic hydrogen, which is 210 μC/cm^2; m is the weight of platinum on the electrode (the weight of platinum was calculated based on the weight of the catalytic layer deposited on the working electrode, taking into account the mass fraction of metals). This approach for the calculation of the ESA value is successfully used not only for Pt/C, but also for bimetallic catalysts [28]. In addition, for bimetallic catalysts, a good correlation between the ESA values measured independently by the adsorption/desorption of an atomic hydrogen monolayer and by the estimation of the area based on the oxidation of a chemisorbed CO monolayer was shown [18–19].

The activity of catalysts in MOR was evaluated in 0.1 M $HClO_4$ with the addition of 0.5 M CH_3OH with a potential sweep rate of 20 mV/s. At the same time, for the estimation of the activity in MOR, the generally accepted characteristics of cyclic voltammograms [29], are: Q_{CH3OH} is the amount of electricity used for the oxidation of methanol in the forward potential sweep; I_{Max} is the maximum current density in the forward potential sweep. For the assessment of the tolerance of catalysts to intermediate products of methanol oxidation, chronoamperograms were recorded under similar conditions at a potential of 0.87 for 30 min. The potential of 0.87 V corresponds to the potential of the direct peak of methanol oxidation. An increase in the polarizing potential is impractical due to the formation of passivating oxide compounds on the surface of the electroactive catalyst particles, which, along with the adsorption of the oxidation product, carbon monoxide, can be the cause of the observed current drop in the chronoamperograms. For the assessment of the tolerance, the following coefficients were calculated: $K = \frac{I_\mathrm{initial}}{I_\mathrm{final}} \cdot 100\%$ is the degree of residual current after 30 min, where I_initial and I_final are the initial and final current densities on the chronoamperogram, respectively, and $\delta = \frac{100}{I_0} \cdot (dI/dt)_{t>500}$ is the coefficient of long-term CO poisoning [30], taking into account the slope of the curve, where I_0 is the current density at the beginning of polarization inversely extrapolated from the linear decay of the current, $(dI/dt)_{t>500}$ is the slope of the linear attenuation of the current.

For the assessment of the stability of the obtained catalysts, we chose the mode of multiple cycling (1000 cycles) in the potential range of 0.4–1.6 V with a potential sweep rate of 100 mV/s [31]. Upon completion of stress testing in

the electrochemical cell, 0.5 M CH_3OH was added to the electrolyte and cyclic voltammograms and chronoamperograms were reordered. The stability of the catalysts in MOR was evaluated by comparing the parameters characterizing the activity and tolerance of materials. All potentials in this study are shown relative to a reversible hydrogen electrode (RHE).

3. Results and discussion

2.1. Study of the composition and structure of PtCuAu/C materials

The mass fraction of metals in the obtained catalysts turned out to be close to the calculated value (40 wt%) and amounted to 34–37 wt%. Table 1). The wide reflection maximum within an angle range of 2θ about 41° on the X-ray diffraction pattern of the PtCu/C catalyst (Fig. 1a) was shifted to the region of large values of angles 2θ (Fig. 1), as compared to the platinum phase (2θ = 39.8°), which was due to the formation of a solid PtCu solution. With the subsequent galvanic substitution of part of the copper for gold, a smaller shift of the Pt (111) maximum was observed in the X-ray diffraction pattern, compared to the PtCu/C material, which may be due to the formation of a PtCuAu solid solution, since the lattice parameter of gold (3.83 Å) is larger than that of platinum and copper. The similar position of the maximum was demonstrated for the PtCuAu/C_A material obtained by the co-reduction of precursors. For this material, additional weak peaks of the gold phase were also observed in the region of angles 2θ around 38° and 44°, corresponding to Au (111) and Au (200). These maxima indicate the presence of a separate Au phase in the PtCuAu/C_A material and, accordingly, the incomplete incorporation of gold into the composition of the

Table 1. Composition and structural characteristics of the obtained catalysts and commercial Pt/C material

Materials	Composition (XRF)	M-Loading (M), ω %	Average Size of Crystallites D_{Av}, nm (XRD)	Crystal lattice parameter, Å	Average Size of Nanoparticles D_{Av} (NPs), nm (TEM)
PtCu/C	Pt_1Cu_1	37±1	1.9 ± 0.3	3.79	–
PtCuAu/C_G	$Pt_1Cu_{0.51}Au_{0.10}$	34±1	2.0 ± 0.3	3.82	6.5
PtCuAu/C_A	$Pt_1Cu_{0.49}Au_{0.10}$	36±1	2.6 ± 0.3	3.83	2.9
JM20	Pt	40±1	2.0 ± 0.2	3.94	3.6*

* TEM for Pt/C from literature [37]

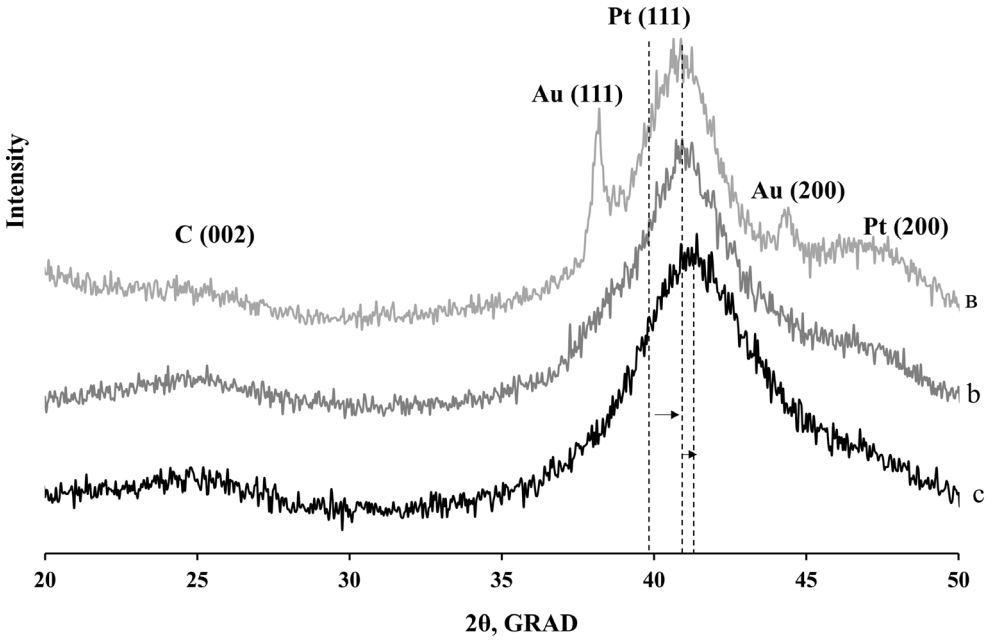

Fig. 1. X-ray diffraction patterns of catalysts: (a) PtCu/C, (b) PtCuAu/C_G, and (c) PtCuAu/C_A

PtCu solid solution. It should be noted that peaks corresponding to the phases of pure copper and its oxides were not revealed in the diffraction patterns of the studied catalysts. Nevertheless, the presence of amorphous structures cannot be ruled out [32]. The average crystallite size for the obtained catalysts, determined using the Scherrer equation, was in the range of 1.9–2.6 nm.

According to the TEM results (Fig. 2), the obtained PtCuAu/C_G and PtCuAu/C_A catalysts were characterized by a uniform distribution of metal NP over the surface of the carbon carrier. For the determination of the average size and size distribution of metal NP, TEM photographs were processed; the size of at least 400 particles was determined for each material. It was found that the average nanoparticle size for the PtCuAu/C_G material was 6.5 nm (Table 1), which is much higher than for the PtCuAu/C_A catalyst, the average particle size of which was 2.7 nm. The PtCuAu/C_A sample was characterized by a narrow size distribution of nanoparticles, while the PtCuAu/C_G sample was characterized by a wide size distribution of NP, from 2 to 12 nm (see histograms in Fig. 2). It should be noted that the average size of NP according to the TEM data for the studied catalysts turned out to be larger than the average size of crystallites calculated using the Scherrer equation (Table 1) [33], which indicates the polycrystalline nature of the particles. Probably, the larger size of NP for the PtCuAu_G catalyst is associated with the larger size of nanoparticles of the initial PtCu/C catalyst, which is due to the peculiarities of the boron hydride synthesis technique. Thus, it was shown in [34] that the PtCu/C material obtained under similar conditions has an average NP size of about 5.5 nm. Probably, the galvanic substitution of gold leads only to an insignificant enlargement of PtCu NP.

The actual composition of the obtained materials turned out to be close to that calculated based on the loading of precursors (Table 1). For the EDX analysis of the elemental composition of individual areas of the surface of PtCuAu/C materials, elemental mapping was used. According to EDX data, the most metal nanoparticles

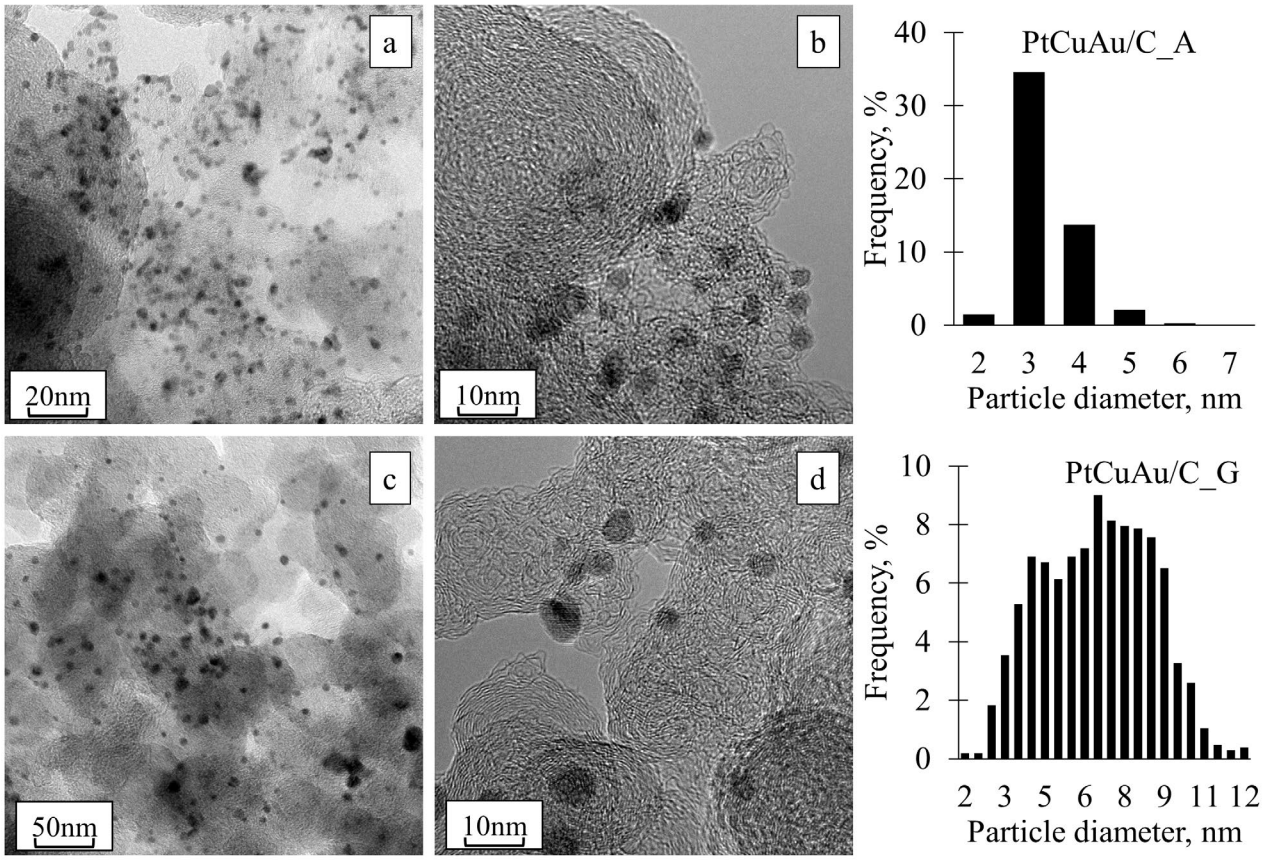

Fig. 2. TEM photographs and histograms of the nanoparticle size distribution obtained on their basis, for samples a,b – PtCuAu/C_A; (c, d) PtCuAu/C_G. 1000 particles of each material were selected for analysis

contained Pt, Cu, and Au atoms. The intensity of the signal from gold atoms was significantly lower, which was due to its lower atomic fraction in the material compared to other metals. For a more detailed analysis, the stencil grid, consisting of ellipses applied to the localizations of Pt (red) and gold (yellow), was transferred to photographs showing the localizations of other metals (Fig. 3). It can be seen from the Figure that all three components were not always included in the composition of the same nanoparticles. For example, in the PtCuAu/C_G material, in addition to trimetallic PtCuAu nanoparticles, bimetallic CuAu nanoparticles were present, since for the yellow ellipses a mismatch in the localization of gold and platinum atoms was revealed. For the PtCuAu/C_A material, the presence of CuAu nanoparticles was not typical (Fig. 3b, Fig. 3c).

2.2. Study of activity and stability of PtCuAu/C catalysts

Electrochemical standardization of the electrodes was carried out before measuring the activity of catalysts by cyclic voltammetry [18–21]. At the stage of electrochemical standardization of the obtained PtCuAu/C catalysts, no peaks of copper dissolution typical for the dissolution of copper from its own phase or the solid solution phase [35–36] were found in cyclic voltammograms in the potential ranges of 0.25–0.45 V and 0.70–0.80 V relative to RHE. Probably, this was due to the absence of the copper phase on the surface of the nanoparticles or on the carbon carrier and indicated a rather complete incorporation of copper into the solid solution. On the other hand, the absence of copper dissolution peaks in cyclic voltammograms does not disprove the possibility of the presence of X-ray amorphous copper oxide.

After standardization of the surface of the materials, cyclic voltammograms were recorded (Fig. 4), the hydrogen region of which was used to determine the ESA value of the catalyst based on the electrochemical adsorption/desorption of hydrogen atoms. The ESA values for PtCu/C and

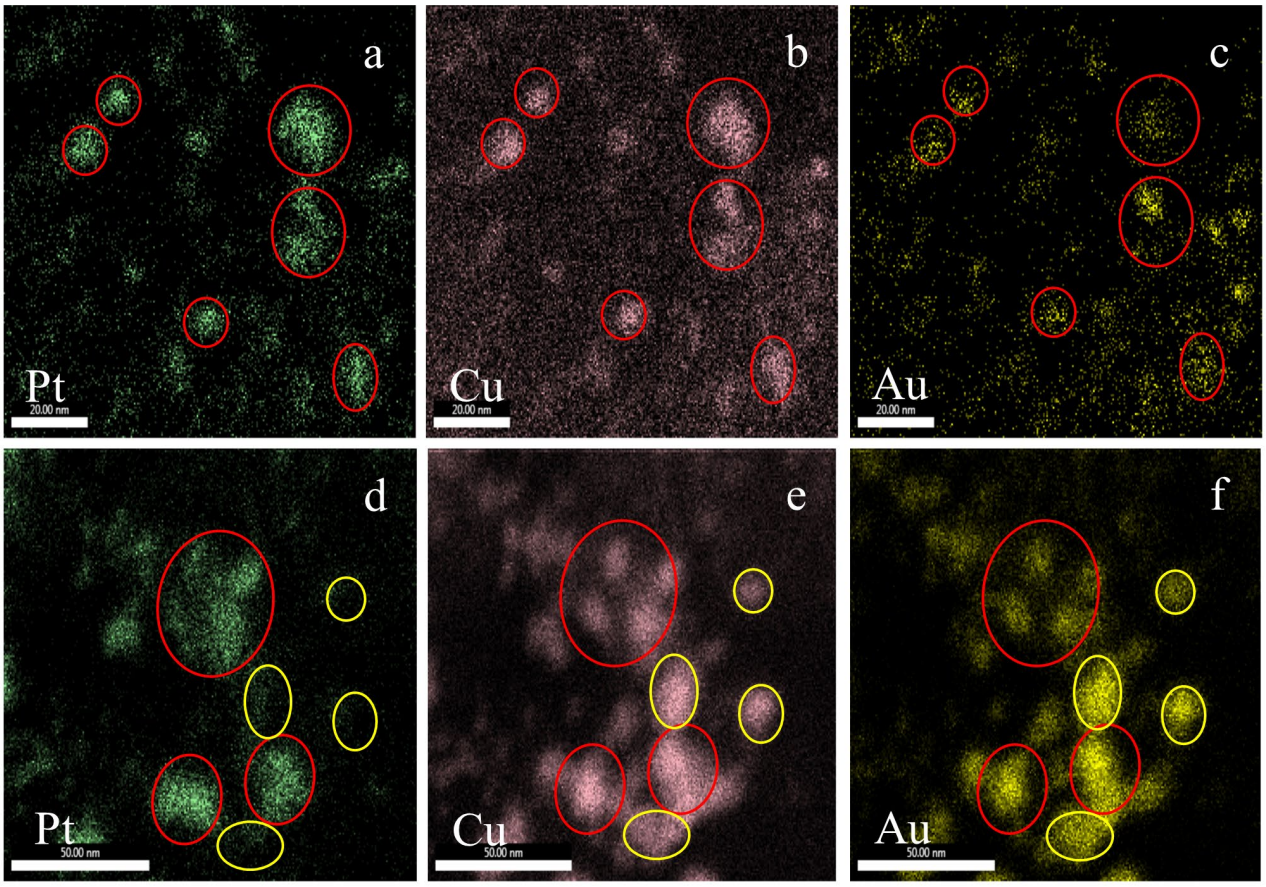

Fig. 3. EDX mapping of a,b,c - PtCuAu/C_A and d,e,f - PtCuAu/C_G catalysts

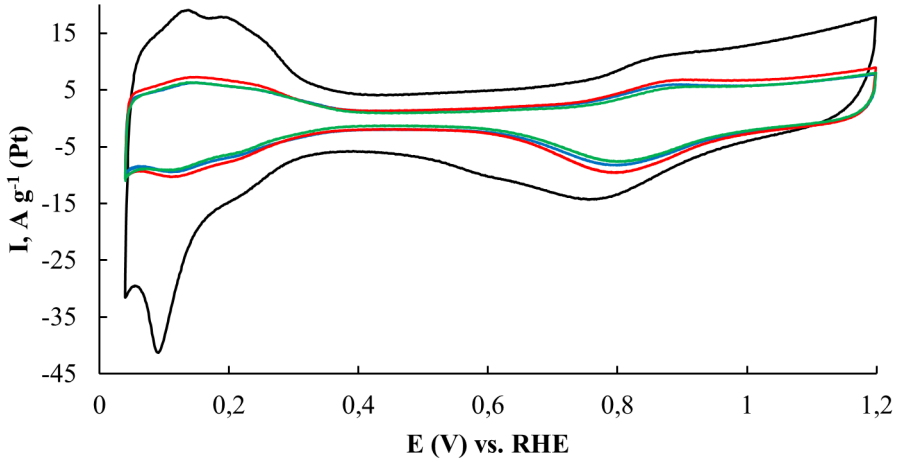

Fig. 4. Cyclic voltammograms of catalysts. Electrolyte is 0.1 M $HClO_4$, Ar atmosphere. The potential sweep rate is 20 mV s^{-1}

Table 2. Values of electrochemically active surface and catalyst activity in methanol

Materials	Q_{CH3OH}, C/g(Pt) 10^5	ESA, m^2/g(Pt)	I_{max}, A/g(Pt)	*I* chronoamperograms, A/g(Pt)		Long-term poisoning rate CO δ, %/s
				$I_{initial}$	I_{final}	
PtCu/C	43	28 ± 3	380	220	48	0.0435
PtCuAu/C_G	59	32 ± 3	572	395	77	0.0481
PtCuAu/C_A	52	31 ± 3	516	331	75	0.0495
JM20	42	77 ± 8	350	320	127	0.0327

PtCuAu/C materials were noticeably inferior to the ESA value calculated for the commercial Pt/C analogue (Table 2). In the case of the PtCuAu/C_G sample, the lower ESA value can be explained by the significantly larger size and wide size distribution of nanoparticles compared to the commercial Pt/C material. At the same time, the particle size of the PtCuAu/C_A material according to TEM slightly differs from that for the Pt/C catalyst. Possibly, the lower ESA value was due to the substitution of a proportion of the platinum atoms on the surface of the catalyst nanoparticles for gold atoms, which are not characterized by reversible adsorption/desorption of hydrogen, as well as to a higher degree of NP agglomeration due to the used synthesis technique [34]. It should be noted that the ESA value of the PtCuAu/C_G material differs slightly

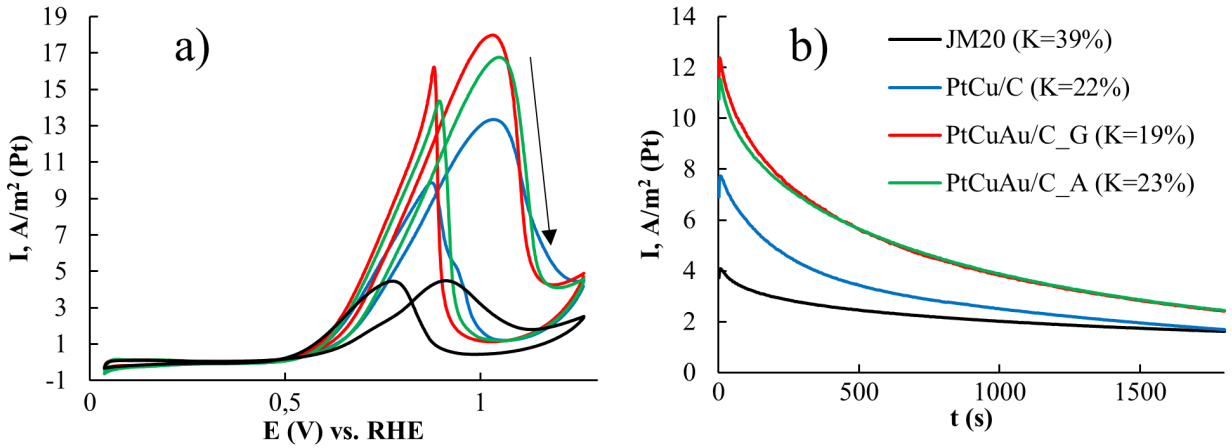

Fig. 5. (a)-cyclic voltammograms and (b) – chronoamperograms at a potential of 0.87 V. Electrolyte is 0.1 M $HClO_4$ + 0.5 M CH_3OH, Ar atmosphere

from the ESA value of the PtCu/C catalyst from which it was obtained. This fact indicates that in the process of galvanic substitution of copper atoms by gold, surface defects do not occur.

The activity of the catalysts in MOR was studied by the method of cyclic voltammograms after the addition of 0.5 M CH_3OH to the electrolyte (Fig. 5a). The PtCuAu/C_G and PtCuAu/C_A materials demonstrated the highest activity in MOR, both per platinum weight in the catalyst and per ESA value (Table 2). At the same time, for the PtCuAu/C_G catalyst, the maximum specific current and the amount of electricity used for the oxidation of methanol in the forward potential sweep among the studied materials were observed. According to the results of chronoamperometric measurements at the potential E = 0.87 V (Fig. 5b, Table 2), the PtCuAu/C_G and PtCuAu/C_A catalysts demonstrate both the highest initial and final specific currents recorded after 30 min at a constant potential compared to PtCu/C and Pt/C materials. At the same time, PtCu/C and both PtCuAu/C catalysts were characterized by a larger relative drop in currents with time (Fig. 5b), reflected in the value of the K coefficient (Figs. 5b, 6b). The long-term CO poisoning coefficient (δ) considers the current decay with time and will have the lowest value for catalysts for which the difference between the initial and final currents is close. Indeed, the CO poisoning coefficient was the lowest for the commercial Pt/C material. Probably, the lowest value of the coefficient for the Pt/C sample was since already after 500 sec of the experiment, the current reached a practically constant value, which indicates a high tolerance of the catalyst to the intermediate products of methanol oxidation. Accelerated stress testing of PtCu/C and PtCuAu/C catalysts in a three-electrode cell revealed that the highest current value per platinum weight after 30 min of the experiment was observed for the Pt/C catalyst (Table 2). Thus, doping of platinum with copper and gold atoms led to an increase in the catalytic activity in the methanol oxidation reaction, but at the same time caused a decrease in the tolerance of materials to poisoning by intermediate products.

The study of catalyst stability in accelerated stress testing showed that bi- and trimetallic catalysts degrade less than the commercial Pt/C analogue. This was clearly seen by comparison of ESA values after completion of the tests (Table 3). Thus, ESA decreased by 18% for PtCuAu/C_G, by 38% for PtCuAu/C_A, and by 33% for PtCu/C. At the same time, for the commercial Pt/C (JM20) catalyst, the reduction in ESA was 78%. The fact that after the completion of stress testing, both the weight and specific activity in MOR turned out to be the highest for the PtCuAu/C_G catalyst is even more important (Fig. 6a, Table 3). The same catalyst, PtCuAu_G, demonstrated the highest tolerance to methanol conversion products (Fig. 6b, Table 3). The tendency towards a decrease in the poisoning coefficient, observed for bi- and trimetallic materials after stress testing also should be mentioned.

4. Conclusions

Based on the results of evaluation of the catalytic activity, stability, and tolerance to intermediate products of methanol oxidation of the obtained catalysts by cyclic voltammetry and chronoamperometry, it was found that, despite the lower values of ESA compared to commercial Pt/C analogue, bi- and trimetallic catalysts have the highest activity in MOR.

It was established that a small addition of gold can increase the activity of the initial PtCu/C catalyst in MOR. The tolerance to the intermediate products of methanol oxidation for

Table 3. Values of electrochemically active surface and catalyst activity in methanol after stress testing

Materials	Q_{CH3OH}, C/g(Pt)·10^5	ESA, m^2/g(Pt)	I_{max}, A/g(Pt)	I chronoamperograms, A/g(Pt)		Long-term poisoning rate CO δ, %/s
				$I_{initial}$	I_{final}	
PtCu/C	21	19 ± 2	235	216	11	0.0333
PtCuAu/C_G	37	26 ± 3	370	284	71	0.0394
PtCuAu/C_A	19	19 ± 3	216	207	14	0.0353
JM20	4	17 ± 8	50	86	3	0.0499

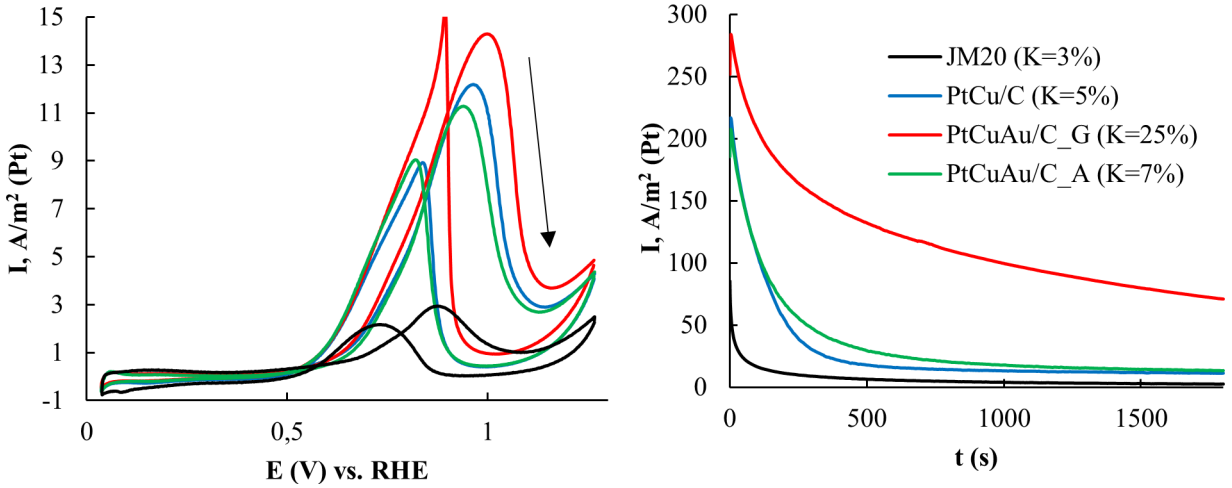

Fig. 6. (a)-cyclic voltammograms and (b)- chronoamperograms at a potential of 0.87 V after stress testing in an electrochemical cell. Electrolyte is 0.1 M $HClO_4$ + 0.5 MCH_3OH, Ar atmosphere

the obtained catalysts turned out to be lower than that of the Pt/C material, which may be due to the lowest ESA values. With a smaller ESA value of the material, the same amount of methanol was oxidized over a smaller surface area and the amount of oxidized methanol was greater per unit surface area. This results in higher surface poisoning compared to materials with higher ESA values. However, after the completion of stress testing, the activity and tolerance for the obtained trimetallic catalysts turned out to be an order of magnitude higher than for the Pt/C (JM20) material. Among the studied catalysts, the PtCuAu/C_G catalyst demonstrated the highest activity and tolerance in MOR after stress testing, which was 7.5 times higher than the Pt/C (JM20) material. The trimetallic PtCuAu/C_A and PtCuAu/C_G catalysts obtained by different synthesis methods demonstrated comparable activity in MOR; however, after stress testing, the PtCuAu/C_G material significantly outperformed the PtCuAu/C_A catalyst in terms of activity. This fact may be related to the large size of trimetallic nanoparticles for PtCuAu/C_G compared to PtCuAu/C_A, which ensures greater stability of this material according to the results of stress testing. For example, in [14], the PtCuAu/C material exhibits an activity 4.5 times higher than the commercial Pt/C. Thus, trimetallic catalysts are of interest for further study and testing in MEA. An important issue that needs to be addressed for testing is the prevention of copper dissolution during the MEA operation. One of the ways to solve this problem, along with the substitution of atoms copper by gold, is the pre-treatment of obtained catalysts in acids.

Author contributions

All authors made an equivalent contribution to the preparation of the publication.

Conflict of interests

The authors declare that they have no known competing financial interests or personal relationships that could have influenced the work reported in this paper.

References

1. Alias M. S., Kamarudin S. K., Zainoodin A. M., Masdar M. S. Active direct methanol fuel cell: An overview. *International Journal of Hydrogen Energy*. 2020;45(38): 19620–19641. https://doi.org/10.1016/j.ijhydene.2020.04.202

2. Gwak G., Kim D., Lee S., Ju H. Luo Y., Zhao J. Studies of the methanol crossover and cell performance behaviors of high temperature-direct methanol fuel cells (HT-DMFCs). *International Journal of Hydrogen Energy*. 2018;43(30): 13999–14011. https://doi.org/10.1016/j.ijhydene.2017.11.029

3. Hamnett A. Mechanism and electrocatalysis in the direct methanol fuel cell. *Catalysis Today*. 1997;38(4): 445–457. https://doi.org/10.1016/S0920-5861(97)00054-0

4. Wu M., Wu X., Zhang L., Abdelhafiz A., Chang I., Qu C., Jiang Y., Zeng J., Alamgir F. Cu@Pt catalysts prepared by galvanic replacement of polyhedral copper nanoparticles for polymer electrolyte membrane fuel cells. *Electrochimica Acta*. 2019;306: 167–174. https://doi.org/10.1016/j.electacta.2019.03.111

5. Qian J., Wei W., Huang X., Tao Y., Chen K., Tang X. A study of different polyphosphazene-coated carbon nanotubes as a Pt–Co catalyst support for methanol oxidation fuel cell. *Journal of Power Sources*. 2012;210: 345–349. https://doi.org/10.1016/j.jpowsour.2012.03.012

6. Fang B., Liu Z., Bao Y., Feng L. Unstable Ni leaching in MOF-derived PtNi-C catalyst with improved performance for alcohols fuel electro-oxidation. *Chinese Chemical Letters*. 2020;31(9): 2259–2262. https://doi.org/10.1016/j.cclet.2020.02.045

7. Mansor M., Timmiati S, Lim K, Wong W, Kamarudin S. K., Kamarudin N. H. N. Recent progress of anode catalysts and their support materials for methanol electrooxidation reaction. *International Journal of Hydrogen Energy*. 2019;44: 14744-69. https://doi.org/10.1016/j.ijhydene.2019.04.100

8. An X.-S., Fan Y.-J., Chen D.-J., Wang Q., Zhou Z.-Y., Sun S.-G. Enhanced activity of rare earth doped PtRu/C catalysts for methanol electro-oxidation. *Electrochimica Acta*. 2011;56(24): 8912–8918. https://doi.org/10.1016/j.electacta.2011.07.106

9. Sulaiman J, Zhu S, Xing Z, Chang Q, Shao M. Pt-Ni octahedra as electrocatalysts for ethanol electro-oxidation reaction. *ACS Catalysis*. 2017;7: 5134–5141. https://pubs.acs.org/doi/10.1021/acscatal.7b01435

10. Page T, Johnson R, Hormes J, Noding S, Rambabu B. A study of methanol electro-oxidation reactions in carbon membrane electrodes and structural properties of Pt alloy electrocatalysts by EXAFS. *Journal of Electroanalytical Chemistry*. 2000;485: 34–41. https://doi.org/10.1016/S0022-0728(00)00090-5

11. Baronia R, Goel J, Tiwari S, Singh P. Efficient electro-oxidation of methanol using PtCo nanocatalysts supported reduced graphene oxide matrix as anode for DMFC. *International Journal of Hydrogen Energy*. 2017;42:10238–10247. https://doi.org/10.1016/j.ijhydene.2017.03.011

12. Markovic N, Gasteiger H, Ross P, Jiang X, Villegas I., Weaver M.J. Electro-oxidation mechanisms of methanol and formic acid on Pt–Ru alloy surfaces. *Electrochimica Acta*. 1995;40: 91-8. https://doi.org/10.1016/0013-4686(94)00241-R

13. Wang X., Zhang L., Wang F., Yu J., Zhu H. Nickel-introduced structurally ordered PtCuNi/C as high performance electrocatalyst for oxygen reduction reaction. *Progress in Natural Science: Materials International*. 2020;30(6): 905–911. https://doi.org/10.1016/j.pnsc.2020.10.017

14. Wang X., Zhang L., Gong H., Zhu Y., Zhao H., Fu Y. Dealloyed PtAuCu electrocatalyst to improve the activity and stability towards both oxygen reduction and methanol oxidation reactions. *Electrochimica Acta*. 2016;212: 277–285. https://doi.org/10.1016/j.electacta.2016.07.028

15. Sarkar A., Murugan A. V., Manthiram A. Rapid microwave-assisted solvothermal synthesis of methanol tolerant Pt-Pd-Co nanoalloy electrocatalysts. *Fuel Cells*. 2010;10(3): 375–383. https://doi.org/10.1002/fuce.200900139

16. Srivastava R., Mani P., Hanh N., Strasser P. Efficient oxygen reduction fuel cell electrocatalysis on voltammetrically dealloyed Pt-Cu-Co nanoparticles. *Angewandte Chemie - International Edition*. 2007;46(47): 8988–8991. https://doi.org/10.1002/anie.200703331

17. Khatib F. N., Wilberforce T., Ijaodola O., Ogungbemi E., El-Hassan Z., Durrant A., Thompson J., Olabi A.G., Material degradation of components in polymer electrolyte membrane (PEM) electrolytic cell and mitigation mechanisms: *Renewable and Sustainable Energy Reviews*. 2019;111: 1–14. https://doi.org/10.1016/j.rser.2019.05.007

18. Belenov S. V., Men'shchikov V. S., Nikulin A. Y., Novikovskii N. M. PtCu/C materials doped with different amounts of gold as the catalysts of oxygen electroreduction and methanol electrooxidation. *Russian Journal of Electrochemistry*. 2020;56(8): 660–668. https://doi.org/10.1134/S1023193520080029

19. Belenov S. V., Menschikov V. S., Nevelskaya A. K., Rezvan D. V. Influence of PtCuAu's nanoparticle structure on its activity in methanol oxidation reaction. *Nanotechnol Russia*. 2019;14(11-12): 557–564. https://doi.org/10.1134/S1995078019060028

20. Alekseenko A. A., Guterman V. E., Volochaev V. A., Belenov, S. V. Effect of wet synthesis conditions on the microstructure and active surface area of Pt/C catalysts. *Russ. J. Inorganic Materials*. 2015;51(12): 1258–1263. http://dx.doi.org/10.1134/S0020168515120018

21. Guterman V. E., Belenov S. V., Pakharev A. Yu., Min M., Tabachkova N. Yu., Mikheykina E. B., Vysochina L. L., Lastovina T. A. Pt-M/C (M = Cu, Ag) electrocatalysts with an inhomogeneous distribution of metals in the nanoparticles. *International Journal of Hydrogen Energy*. 2016;41(3): 1609–1626. https://doi.org/10.1016/j.ijhydene.2015.11.002

22. Brugeman S. A., Zekhtor M. Yu., Novikovskiy N. M. *Universal Roentgen Spectra (UniveRS)*. Certificate of state registration of the computer program no. 2010615318 (Russia). 2010.

23. Langford J. I., Wilson A. J. C. Scherrer after Sixty Years: A Survey and Some New Results in the Determination of Crystallite Size. *Journal of Applied Crystallography*. 1978;11: 102–103. https://doi.org/10.1107/S0021889878012844

24. Guterman, V. E., Belenov, S. V., Lastovina, T. A., Fokina, E. P., Prutsakova, N. V., Konstantinova, Y. B. Microstructure and electrochemically active surface area of PtM/C electrocatalysts. *Russian Journal of Electrochemistry*. 2011;47(8) 997–1004. https://doi.org/10.1134/S1023193511080052

25. Groger O., Gasteiger H. A., Suchsland J. P. Review—Electromobility: Batteries or Fuel Cells? *Journal of The Electrochemical Society*. 2015;162(14): 2605–2623. http://dx.doi.org/10.1149/2.0211514jes

26. Garsany Y., Ge J., St-Pierre J., Rocheleau R., Swider-Lyons K. Analytical procedure for accurate comparison of rotating disk electrode results for the oxygen reduction activity of Pt/C. *Journal of The Electrochemical Society*. 2014;161(5): 628–640. http://dx.doi.org/10.1149/2.036405jes

27. Banham D., Ye S. Current status and future development of catalyst materials and catalyst layers for proton exchange membrane fuel cells: An industrial perspective. *ACS Energy Letters*. 2017;2(3): 629–638. https://doi.org/10.1021/acsenergylett.6b00644

28. Zhang C., Zhang Y., Xiao H., Zhang J., Li L., Wang L., Bai Q., Liu M., Wang Z, Sui N. Superior catalytic performance and CO tolerance of PtCu/graphdiyne electrocatalyst toward methanol oxidation reaction. *Colloids and Surfaces A: Physicochemical and Engineering Aspects*. 2021;612: 125960. https://doi.org/10.1016/j.colsurfa.2020.125960

29. Menshikov V. S., Novomlincky I. N., Belenov S. V., Alekseenko A. A., Safronenko O. I., Guterman V. E. Methanol, ethanol, and formic acid oxidation on new platinum-containing catalysts. *Catalysts*. 2021;11(2): 158–176. https://doi.org/10.3390/catal11020158

30. Guo J. W., Zhao T. S., Prabhuram J., Chen R., Wong C. W. Preparation and characterization of a PtRu/C nanocatalysts for direct methanol fuel cell. *Electrochimica Acta*. 2005;51(4): 754–763. https://doi.org/10.1016/j.electacta.2005.05.056

31. Shao Y., Yin G., Gao Y. Understanding and approaches for the durability issues of Pt-based catalysts for PEM fuel cell. *Journal of Power Sources*. 2007;171(2): 558–566. https://doi.org/10.1016/j.jpowsour.2007.07.004

32. Pryadchenko V. V., Srabionyan V. V., Kurzin A. A., Bulat N. V., Shemet D. B., Avakyan L. A., Belenov S. V., Volochaev V. A., Zizak I., Guterman V. E., Bugaev L. A. Bimetallic PtCu nanoparticles in PtCu/C electrocatalysts: structural and electrochemical characterization. *Applied Catalysis A: General*. 2016;525: 226–236. https://doi.org/10.1016/j.apcata.2016.08.008

33. Guterman V. E., Belenov S. V., Alekseenko A. A., Lin R., Tabachkova N. Y., Safronenko O. I. Activity and stability of Pt/C and Pt-Cu/C. *Electrocatalysts*. 2018;9(5): 550–562. https://doi.org/10.1007/s12678-017-0451-1

34. Guterman V. E., Belenov S. V., Alekseenko A. A., Volochaev V. A., Tabachkova N. Y. The relationship between activity and stability of deposited platinum-carbon electrocatalysts. *Russian Journal of Electrochemistry*. 2017;53(5): 531–539. https://doi.org/10.1134/S1023193517050081

35. Zhu H., Li X., Wang F. Synthesis and characterization of Cu@Pt/C core-shell structured catalysts for proton exchange membrane fuel cell. *International Journal of Hydrogen Energy*. 2011;36(15) 9151–9154. https://doi.org/10.1016/j.ijhydene.2011.04.224

36. Wang Y., Zhou H., Sun P., Chen T. Exceptional methanol electro-oxidation activity by bimetallic concave and dendritic Pt-Cu nanocrystals catalysts. *Journal of Power Sources*. 2014;245(1): 663–670. https://doi.org/10.1016/j.jpowsour.2013.07.015

37. Na H., Choi H., Oh J. W., Jung Y. S., Cho Y. S. Enhanced CO oxidation and cyclic activities in three-dimensional platinum/indium tin oxide/carbon black electrocatalysts processed by cathodic arc deposition. *ACS Applied Materials and Interfaces*. 2019;11(28): 25179–25185. https://doi.org/10.1021/acsami.9b06159

Information about the authors

Vldislav S. Menshikov, PhD student, Researcher at the Department of Electrochemistry, Southern Federal University (Rostov-on-Don, Russian Federation).

https://orcid.org/0000-0002-0531-2156

men.vlad@mail.ru.

Sergey V. Belenov, PhD in Chemistry, Research Fellow at the Department of Electrochemistry, Southern Federal University (Rostov-on-Don, Russian Federation).

https://orcid.org/0000-0003-2980-7089

serg1986chem@mail.ru

Aleksey Y. Nikulin, Researcher at the Department of Electrochemistry, Southern Federal University (Rostov-on-Don, Russian Federation;).

chemistnik@yandex.ru

Received August 22, 2021; approved after peer reviewing December 7, 2021; accepted for publication February 15, 2022; published online March 25, 2022.

Translated by Valentina Mittova

Edited and proofread by Simon Cox